LBP Histogram Selection based on Sparse Representation for Color Texture Classification

Vinh Truong Hoang, Alice Porebski, Nicolas Vandenbroucke and Denis Hamad
Laboratoire d'Informatique Signal et Image de la Côte d'Opale,
50, rue Ferdinand Buisson, BP 719, 62228 Calais Cedex, France
truong@lisic.univ-littoral.fr

Keywords: Histogram Selection, Feature Selection, LBP Color Histogram, Texture Classification, Sparse Representation.

Abstract: In computer vision fields, LBP histogram selection techniques are mainly applied to reduce the dimension of color texture space in order to increase the classification performances. This paper proposes a new histogram selection score based on Jeffrey distance and sparse similarity matrix obtained by sparse representation. Experimental results on three benchmark texture databases show that the proposed method improves the performance of color texture classification represented in different color spaces.

1 INTRODUCTION

Texture classification is a fundamental task in image processing and computer vision. It is an important step in many applications such as content-based image retrieval, face recognition, object detection and many more. Texture analysis methods was firstly designed for dealing with gray-scale images. Among the proposed approaches in the recent years to represent the texture images, Local Binary Pattern (LBP) proposed by Ojala et al. has been known as one of the most successful statistical approaches due to its efficacy, robustness against illumination changes and relative fast calculation (Ojala et al., 1996; Ojala et al., 2001; Pietikäinen et al., 2002; Ojala et al., 2002b). In order to encode LBP, the gray level of each pixel is compared with those of its neighbors and the results of these comparisons are weighted and summed. The obtained texture feature is the LBP histogram whose bin count depends on the number of neighbors.

Otherwise, it has been demonstrated that color information is very important to represent the texture, especially natural textures (Asada and Matsuyama, 1992). However, the extension of LBP to color leads to consider several LBP histograms and only some of which are relevant for texture classification. That is the reason why many approaches have been proposed to reduce the dimension of the feature space based on the LBP histogram in order to improve the classification performances (Zhang and Xu, 2015; Porebski et al., 2013b; Guo et al., 2012; Zhou et al., 2013b; Mehta and Egiazarian, 2016; Ren et al., 2015). The dimensionality reduction consists to select the pertinent histogram bins. Another dimensional reduction method was proposed by Porebski et al. which focus on selecting LBP histograms in their entirety. For this purpose they introduce the Intra-Class Similarity score (ICS-score) based on the similarity of the textures within the different classes (Porebski et al., 2013a). Kalakech et al. introduced another histogram selection score, named "Adapted Supervised Laplacian score" (ASL-score) based on Jeffrey distance and a similarity matrix (Kalakech et al., 2015). This matrix is deduced from the class labels. It is a hard value which is 0 or 1.

In this paper, we propose to extend the ASL-score by using sparse representation to build a soft similarity matrix that takes values between 0 and 1. Indeed, in the past few years, sparse representation has been successfully applied in signal and image processing fields and proven to be an effective tool for feature selection (Qiao et al., 2010; Xu et al., 2013; Zhou et al., 2013a). Moreover, the soft value of the similarity obtained by the sparse representation could better reflect the geometric structure of different classes. Indeed a value between 0 and 1 will measure the similarity in a subtle way, instead of being binary with just two values 0 and 1. This may lead to more powerful discriminating information. The proposed score, called Sparse Adapted Supervised Laplacian score (SpASL-score) will be evaluated thanks to several benchmark color texture databases represented in different color spaces.

In the following, we describe, in section 2, the

Hoang V., Porebski A., Vandenbroucke N. and Hamad D.
LBP Histogram Selection based on Sparse Representation for Color Texture Classification.
DOI: 10.5220/0006128204760483
In *Proceedings of the 12th International Joint Conference on Computer Vision, Imaging and Computer Graphics Theory and Applications (VISIGRAPP 2017)*, pages 476-483
ISBN: 978-989-758-225-7

color LBP histograms. Section 3 presents the histogram selection approach and introduce the ASL-score, while section 4, presents sparse representation for histogram selection and the proposed SpASL-score. In section 5, experimental results indicate that our score achieves better performances than previous works under several benchmark color texture databases.

2 COLOR LBP HISTOGRAM

The LBP operator has been introduced by Ojala et al. in 1996 to describe the textures present in gray-scale images (Ojala et al., 1996). An extension to color images is proposed by Mäenpää et al. and used in several color texture classification problems (Mäenpää and Pietikäinen, 2004; Pietikäinen et al., 2011). The color information of a pixel is characterized by three color component in a 3-dimensional color space, denoted here $C_1C_2C_3$. The color LBP operator consists in assigning to each pixel a label which characterizes the local pattern in a neighborhood. Each label is a binary number calculated by thresholding the color component of the neighbors by using the color component of the considered pixel. The result of the thresholding, performed for each neighbor pixel, is then coded by a weight mask. As do Ojala et al. when they introduce the original LBP operator, the 3×3 pixels neighborhood is considered. To characterize the local pattern of the considered pixel, the weighted values are finally summed so that each label ranges from 0 to 255. In order to characterize the whole color texture image, the LBP operator is applied on each pixel and for each pair of components. The corresponding distributions are thus represented in nine different histograms: three within-component LBP histograms $((C_1,C_1),(C_2,C_2)$ and $(C_3,C_3))$ and six between-component LBP histograms $((C_1,C_2),(C_2,C_1),(C_1,C_3),(C_3,C_1),(C_2,C_3)$ and $(C_3,C_2))$. A color texture is thus represented in a (9×256)-dimensional feature space. This results in a high dimensional space, which could decrease the classification performance. For this, it would be interesting to find the most relevant histograms.

3 HISTOGRAM SELECTION APPROACH

Histogram selection approaches are usually grouped in three ways: filters, wrappers and embedded. The latter combines the reduction of processing time of a filter approach and the high performances of a wrapper approach. Filter approaches consist in computing the score of each histogram in order to measure its efficiency. Then, the histograms are ranked according to the proposed score. In wrapper approaches, histograms are evaluated thanks to a specific classifier and the selected ones are those which maximizes the classification rate.

In the considered LBP histogram selection context, the database is composed of N color texture images, each ones is characterized by 9 histograms. This leads to 9 matrices $\mathbf{H}^r$, which are defined by:

$$\mathbf{H}^r = \left[\mathbf{h}_1^r ... \mathbf{h}_i^r ... \mathbf{h}_N^r\right] = \begin{bmatrix} h_1^r(0) & ... & h_i^r(0) & ... & h_N^r(0) \\ ... & ... & ... & ... & ... \\ h_1^r(k) & ... & h_i^r(k) & ... & h_N^r(k) \\ ... & ... & ... & ... & ... \\ h_1^r(Q) & ... & h_i^r(Q) & ... & h_N^r(Q) \end{bmatrix} \quad (1)$$

where, $r = 1,2,..,9$ and Q being the quantization level.

Several measures have been proposed for evaluating difference between two histograms like Kullback-Leibler, χ^2, earth movers, Jeffrey, etc. (Cha and Srihari, 2002). Jeffrey distance has the advantage of being positive and symmetric. It is defined by:

$$J(\mathbf{h}_i^r, \mathbf{h}_j^r) = \sum_{k=1}^{Q} h_i^r(k) log\left(\frac{h_i^r(k)}{\frac{h_i^r(k)+h_j^r(k)}{2}}\right) + \sum_{k=1}^{Q} h_j^r(k) log\left(\frac{h_j^r(k)}{\frac{h_i^r(k)+h_j^r(k)}{2}}\right) \quad (2)$$

In (Kalakech et al., 2015), the Jeffrey distance is used to construct an Adapted Laplacian score ASL^r of the r^{th} histogram:

$$ASL^r = \frac{\sum_{i=1}^{N}\sum_{j=1}^{N} J(\mathbf{h}_i^r, \mathbf{h}_j^r) s_{ij}}{\sum_{i=1}^{N} J(\mathbf{h}_i^r, \overline{\mathbf{h}}^r) d_i} \quad (3)$$

$\overline{\mathbf{h}}^r$ is the histogram average:

$$\overline{\mathbf{h}}^r = \frac{\sum_{i=1}^{N} h_i^r d_i}{\sum_{i=1}^{N} d_i} \quad (4)$$

where, d_i is the local density of image I_i defined by:

$$d_i = \sum_{j=1}^{N} s_{ij} \quad (5)$$

where, s_{ij} is an element of the similarity matrix $\mathbf{S}$. In a supervised context, for each image I_i, a class label is associated y_i. The similarity between two images I_i and I_j is defined by:

$$s_{ij} = \begin{cases} 1 & \text{if } y_i = y_j, \\ 0 & \text{otherwise} \end{cases} \quad (6)$$

In the next section, instead of using hard similarity s_{ij} labels, we will define the similarity matrix from the sparse representation, and then integrate it into the Equation (3).

4 SPARSE REPRESENTATION FOR HISTOGRAM SELECTION

Recently, many works have been focused on sparse linear representation to characterize data (Zhou et al., 2013a; Xu et al., 2013; Zhu et al., 2013). The sparse representation is based on the hypothesis that each image is reconstructed through a linear combination of other images of the database. The modified sparse representation based on l_1-norm minimization problem is used to construct the l_1-graph adjacency structure and a sparse similarity matrix automatically. In (Qiao et al., 2010; Liu and Zhang, 2014) the sparse representation is applied to feature selection in unsupervised and supervised contexts. In this section, we propose to use sparse similarity matrix combined with Jeffrey distance for histogram selection in the supervised context.

4.1 Sparse Similarity Matrix

The modified sparse representation framework has been proposed in order to construct a sparse similarity matrix by finding the most compact representation of data (Qiao et al., 2010). Given an image I_i, characterized by histograms $\mathbf{h}_i^r$, $r = 1,2,..9$, and a histogram matrix $\mathbf{H}^r$ of Equation 1 contains the elements of an over-complete dictionary in its columns. The goal of sparse representation of $\mathbf{h}_i^r$ is to estimate by using a few entries of $\mathbf{H}^r$ as possible.

$$\min_{\mathbf{s}_i} \|\mathbf{s}_i\|_1, \qquad s.t. \quad \mathbf{h}_i^r = \mathbf{H}^r \mathbf{s}_i, \quad 1 = \mathbf{1}^T s_i, \quad (7)$$

where $\mathbf{s}_i \in \Re^N$ is the coefficient vector. It is defined as:

$$\mathbf{s}_i = [s_{i,1}, ..., s_{i,i-1}, 0, s_{i,i+1}, ..., s_{i,N}]^T \quad (8)$$

$\mathbf{s}_i$ is an N-dimensional vector in which the i^{th} element is equal to zero implying that $\mathbf{h}_i^r$ is removed from $\mathbf{H}^r$. $\|\mathbf{s}_i\|_1$ is the l_1-norm of $\mathbf{s}_i$ and $\mathbf{1} \in \Re^N$ is a vector of all ones.

For each sample $\mathbf{h}_i^r$, we can compute the similarity vector $\hat{\mathbf{s}}_i$, and then get the sparse similarity matrix:

$$\mathbf{S} = [\hat{\mathbf{s}}_1, \hat{\mathbf{s}}_2, ..., \hat{\mathbf{s}}_N]^T, \quad (9)$$

where $\hat{\mathbf{s}}_i$ is the optimal solution of Equation (7). The matrix $\mathbf{S}$ determines both graph adjacency structure and sparse similarity matrix simultaneously. Note that, the sparse similarity matrix is generally asymmetric.

Since the real-world images contain noise, the following objective function is used:

$$\min_{\mathbf{s}_i} \|\mathbf{s}_i\|_1, \quad s.t. \quad \|\mathbf{h}_i^r - \mathbf{H}^r \mathbf{s}_i\|_2 < \delta, \quad 1 = \mathbf{1}^T \mathbf{s}_i, \quad (10)$$

where, δ represents the error tolerance which is chosen to 10^{-4} in our experiments. $\|.\|_2$ denotes l_2-norm of a vector. This problem can be solved in a polynomial time with standard linear programming methods (Qiao et al., 2010).

4.2 Sparse Adapted Superived Laplacian Score

In this section, the sparse similarity matrix defined by sparse representation is applied in the supervised context. Given a database of N images belonging to P classes, each class p, $p = 1,..,P$, contains N_p images. For each class, we construct the sparse similarity matrix using images within the same class by Equation (10). We note $\mathbf{S}^p$ the sparse similarity matrix of class p, and h_i^{rp} the r^{th} histogram of image I_i in class p. We notice that the similarity in Equation (6) is hard, it takes the value 1 if the two corresponding images are in the same class and the value 0 if they are in different classes. On the other side, the sparse reconstruction in Equation (10) allows us to determine the soft similarity value between 0 and 1 for two corresponding images. This soft value could then reflect the intrinsic geometric properties of classes which may lead to natural discriminating information.

Integrating the sparse similarity matrix into Equation (3) leads to Sparse Adapted Supervised Laplacian score (SpASL) defined by:

$$SpASL^r = \frac{\sum_{p=1}^{P} \sum_{i,j=1}^{N_p} J(\mathbf{h}_i^{rp}, \mathbf{h}_j^{rp}) \hat{s}_{ij}^p}{\sum_{p=1}^{P} \sum_{i=1}^{N_p} J(\mathbf{h}_i^{rp}, \overline{\mathbf{h}}^{rp}) d_i^p} \quad (11)$$

where, $r = 1,2,...9$ is the histogram index, N_p is the number of images of the p^{th} class, $\hat{s}_{ij}^p$ is the element of the sparse matrix $\mathbf{S}^p$ related to the p^{th} class. Histogram selection consists to compute for each of all 9 histograms the associated SpASL-score and to rank histograms according to their scores in ascending order.

5 EXPERIMENTAL RESULTS

In order to evaluate the efficiency of the proposed score, we perform the evaluation on three bench-

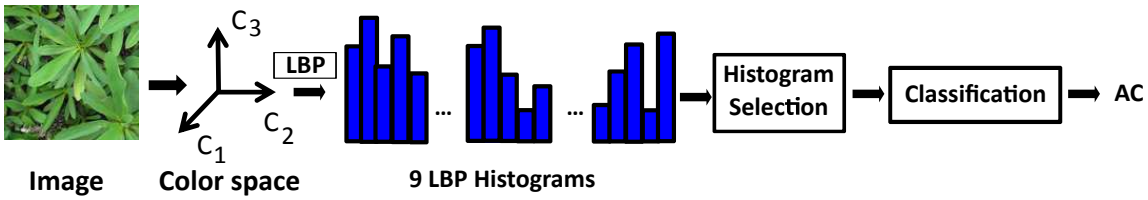

Figure 1: LBP histogram selection scheme.

marks color texture images databases: Outex-TC-0003[1], New BarkTex and USPTex[2]

Note that, each color texture is characterized by 9 LBP histograms. Color texture can be represented in different color spaces, which can be grouped in four families: the primary color spaces, the luminance–chrominance color spaces, the perceptual spaces and the independent axis color spaces (Qazi et al., 2011). In our experiments, we used the following color spaces: RGB, HSV, HLS, ISH, rgb, $b_w r_g b_y$, *I-HLS*, $I_1I_2I_3$, YC_bC_r, *YIQ*, *Luv*, *Lab*, *XYZ*, *YUV*. Figure 1 shows the LBP histogram selection scheme in one color space. In the experiments, we compare our SpASL-score for histogram selection with the original ASL-score proposed in (Kalakech et al., 2015) and the ICS-score proposed in (Porebski et al., 2013b). Each database is divided into training set and testing set, as shown in Table 1. The training set is used for histogram ranking procedure by applying Equation (11). Then, ranked histograms are used as inputs to classification process which is performed based on testing set. The $L1$-distance is associated with 1-*NN* classifier while the classification performance is evaluated by accuracy rate (AC). For every subsection below, we present a short description of the image databases and analyze the obtained experimental results.

5.1 Experiments on BarkTex Database

BarkTex database includes six tree bark classes acquired under natural (daylight) illumination conditions (Lakmann, 1998). The version New Barktex has been built by Porebski et al. (Porebski et al., 2014). Table 2 presents the results on New Barktex database. For each color space, the accuracy rate applied on testing images and the number of the selected LBP histogram reached (in parentheses) are computed. The first rows shows the results obtained by ICS, ASL, SpASL-score and without selection in *RGB* color space. They give exactly the same AC (81.25) with 4 histograms selected. By examining the selected histogram in this color space, we notice that all 3 scores used three within-component LBP histograms (RR, GG, BB) and one between-component LBP histogram (RG). The last row of Table 2 shows the mean AC of 14 color spaces used. We can see that the performance of SpASL-score is slightly higher or equal than ASL-score. The average AC of SpASL-score is better than ICS and ASL-score. The best results obtained is 81.37 by ICS-score in *YIQ* space while ASL and SpASL give the same results. The maximal number of histograms selected is 9 for *Luv* space while the minimal is 2 for *XYZ* and *I-HLS* spaces. It is interesting to note that, ASL and SpASL give within-component LBP histograms as the best score globally while ICS assigns the best score differently. This result can show the effectiveness of sparse similarity matrix given by the proposed score.

5.2 Experiments on Outex-TC-00013 Database

The test suite Outex-TC-00013 is provided by the Outex texture database (Ojala et al., 2002a). This database composes collection of natural materials acquired under three-CCD color camera under the same controlled conditions. Table 3 presents the results on Outex-TC-00013 database.

In most of cases, SpASL gives better results than ASL and ICS, except in $I_1I_2I_3$ color space. The average AC of SpASL-score is better than ICS and ASL-score. The best result (93.38) is reached by *RGB* and *HLS* with 8 histogram selected. The minimal number of histogram selected is 6 for *rgb* and YC_bC_r spaces. As the same for BarkTex database, we notice that SpASL and ASL give within-component LBP histograms as the best score over most of color spaces, except in *Luv* space.

5.3 Experiments on USPTex Database

The USPTex database has textures typically found in daily life, such as beans, rice, tissues, road scenes,

[1]The Outex-TC-0003 image test suite can be downloaded at http://www.cse.oulu.fi/CMV

[2]The BarkTex and USPTex image test suites can be downloaded at https://www.lisic.univ-littoral.fr/˜porebski/Recherche.html

Table 1: Summary of image databases used in experiment.

Dataset name	Image size	# class	# training	# test	Total
New BarkTex (Porebski et al., 2014)	64×64	6	816	816	1632
Outex-TC-00013 (Ojala et al., 2002a)	128×128	68	680	680	1360
USPTex (Backes et al., 2012)	128×128	191	1146	1146	2292

Table 2: Experiments on BarkTex database.

Color space	Without selection	ICS-score	ASL-score	SpASL-score
RGB	73.28 (9)	**81.25** (4)	**81.25** (4)	**81.25** (4)
rgb	74.39 (9)	76.84 (7)	**77.08** (3)	**77.08** (3)
$I_1I_2I_3$	71.69 (9)	**79.53** (7)	**79.53** (7)	**79.53** (7)
HSV	70.47 (9)	**81.00** (3)	**81.00** (3)	**81.00** (3)
$b_w r_g b_y$	72.06 (9)	80.02 (7)	**80.64** (6)	**80.64** (6)
HLS	70.10 (9)	**81.00** (3)	**81.00** (3)	**81.00** (3)
I-HLS	72.06 (9)	75.86 (6)	77.08 (5)	**78.80** (2)
ISH	71.69 (9)	**79.78** (3)	**79.78** (3)	**79.78** (3)
YC_bC_r	71.57 (9)	**79.29** (7)	**79.29** (7)	**79.29** (7)
Luv	71.08 (9)	71.08 (9)	**71.08** (9)	**71.08** (9)
Lab	67.16 (9)	67.65 (7)	**68.14** (6)	**68.14** (6)
XYZ	76.10 (9)	78.19 (3)	78.19 (3)	**78.68** (2)
YUV	71.81 (9)	**78.92** (7)	**78.92** (7)	**78.92** (7)
YIQ	77.08 (9)	**81.37** (6)	80.76 (7)	80.76 (7)
Average	72.18±2.48	77.98±4.04	78.12±3.90	**78.28**±3.89

Table 3: Experiments on Outex-TC-0003 database.

Color space	Without selection	ICS-score	ASL-score	SpASL-score
RGB	92.94 (9)	92.94 (9)	93.24 (8)	**93.38** (8)
rgb	87.06 (9)	87.06 (9)	**87.35** (8)	**87.35** (6)
$I_1I_2I_3$	88.53 (9)	**88.97** (8)	88.68 (6)	88.53 (9)
HSV	90.44 (9)	91.03 (8)	**91.32** (7)	**91.32** (7)
$b_w r_g b_y$	89.95 (9)	89.85 (9)	**91.76** (8)	**91.76** (8)
HLS	92.35 (9)	92.35 (9)	**93.38** (6)	**93.38** (6)
I-HLS	89.71 (9)	89.71 (9)	89.71 (9)	**90.29** (7)
ISH	92.94 (9)	92.94 (9)	**93.09** (8)	**93.09** (8)
YC_bC_r	89.56 (9)	89.56 (9)	**90.59** (8)	**90.59** (6)
Luv	**90.29** (9)	**90.29** (9)	**90.29** (8)	**90.29** (8)
Lab	89.56 (9)	**90.00** (8)	89.85 (6)	89.85 (6)
XYZ	**92.06** (9)	**92.06** (9)	**92.06** (9)	**92.06** (9)
YIQ	88.82 (9)	88.82 (9)	88.97 (8)	**89.26** (8)
YUV	89.56 (9)	89.56 (9)	**90.44** (8)	**90.44** (8)
Average	90.26±1.73	90.36±1.70	90.76±1.81	**90.82**±1.80

... (Backes et al., 2012). The natural color textures images are taken under an unknown but fixed light source. Table 4 presents the results on USPTex database. We can see that, SpASL outperforms the ICS-score and slightly better than ASL-score for all color spaces. The best AC obtained is 93.19 in *YUV* space with only 3 histogram selected. Note that ASL and SpASL-score give within-component LBP histograms as the best score in all color spaces. The results on USPTex confirm again the strength of the

Table 4: Experiments on USPTex database.

Color space	Without selection	ICS-score	ASL-score	SpASL-score
RGB	89.53 (9)	90.31 (6)	**91.27** (4)	**91.27** (4)
rgb	78.36 (9)	**83.25** (3)	**83.25** (3)	**83.25** (3)
$I_1I_2I_3$	75.39 (9)	82.46 (4)	**92.06** (3)	**92.06** (3)
HSV	83.25 (9)	85.78 (7)	**90.40** (3)	**90.40** (3)
$b_w r_g b_y$	77.23 (9)	86.21 (4)	**92.41** (3)	**92.41** (3)
HLS	81.59 (9)	85.08 (7)	**90.31** (3)	**90.31** (3)
I-HLS	83.42 (9)	87.00 (7)	**91.27** (3)	**91.27** (3)
ISH	82.90 (9)	86.04 (7)	**90.40** (3)	**90.40** (3)
YC_bC_r	76.79 (9)	86.74 (4)	**93.11** (3)	**93.11** (3)
Luv	88.74 (9)	88.74 (9)	88.74 (9)	**90.31** (3)
Lab	79.58 (9)	85.78 (7)	85.78 (7)	**87.87** (3)
XYZ	89.79 (9)	90.84 (5)	90.92 (6)	**91.01** (6)
YIQ	76.70 (9)	84.47 (4)	**92.58** (3)	**92.58** (3)
YUV	76.79 (9)	86.04 (4)	**93.19** (3)	**93.19** (3)
Average	81.43.26±5.04	86.38±2.36	90.40±2.82	**90.67**±2.55

Table 5: Classification performance under BarkTex, Outex-TC-00013 and USPTex image databases by histogram selection approaches.

	ICS-score	ASL-score	SpASL-score
BarkTex	**81.37** (6)	81.25 (4)	81.25 (4)
OuTex-TC-0003	92.94 (9)	**93.38** (8)	**93.38** (8)
USPTex	90.84 (5)	**93.19** (3)	**93.19** (3)

Table 6: Classification performance under BarkTex, Outex-TC-00013 and USPTex image databases in the previous works.

Database	Method	Results
BarkTex	Compact descriptors color LBP (Ledoux et al., 2016)	**79.40**
	MCSFS (Porebski et al., 2013b)	75.90
Outex-TC-0003	MCSFS (Porebski et al., 2013b)	**96.60**
	Color histograms (Mäenpää and Pietikäinen, 2004)	95.40
	Parametric spectral analysis (Qazi et al., 2011)	94.50
	Compact descriptors color LBP (Ledoux et al., 2016)	92.50
	Stat multi-model geodesic distance (El Maliani et al., 2014)	89.70
	Block truncation coding (Guo et al., 2016)	88.24
	Colour contrast occurrence matrix (Martínez et al., 2015)	87.79
USPTex	Local jet space (Oliveira et al., 2015)	**94.29**
	Block truncation coding (Guo et al., 2016)	93.94
	Compact descriptors color LBP (Ledoux et al., 2016)	91.90
	Fractal descriptors over the wavelet (Florindo and Bruno, 2016)	85.56

sparse similarity matrix integrated into the proposed score which allows to improve the classification performances.

5.4 Comparison with Previous Existing Methods

Table 6 reports the classification performance with different existing methods in literature under three benchmark image databases. The Multi Color Space

Feature Selection (MCSFS) is used for characterized texture images with 28 color spaces in (Porebski et al., 2013b). The results obtained are 75.90 on BarkTex and 96.60 on OuTex-TC-0003. In (Ledoux et al., 2016), the results obtained are 79.40 on BarkTex, 92.50 on OuTex-TC-0003 and 91.90 on USPTex by using the compact color orders of LBP approach in *RGB* space. By using local jet space, the best results obtained on USPTex is 94.29 in (Oliveira et al., 2015). In order to compare those results, we summarize the best classification performance by histogram selection approaches as shown in Table 5. As we can see, the results obtained by histogram selection is promising by using different single color space.

6 CONCLUSION

Local Binary Pattern (LBP) is one of the most successful approaches to characterize texture images. Its extension to color information is very important to represent natural texture images. However, color LBP leads to consider several histograms, only some of which are pertinent for texture classification. We proposed a histogram selection score based on Jeffrey distance and sparse similarity matrix obtained by sparse representation. Experimental results are achieved with OuTex-TC-00013, BarkTex and USPTex databases. The proposed histogram selection score, integrating soft similarities, improves the results of color texture classification. The works presented in this paper are now continued in order to extend in multi-color space and with different selection strategies.

REFERENCES

Asada, N. and Matsuyama, T. (1992). Color image analysis by varying camera aperture. In *Pattern Recognition, 1992. Vol.I. Conference A: Computer Vision and Applications, Proceedings., 11th IAPR International Conference on*, pages 466–469.

Backes, A. R., Casanova, D., and Bruno, O. M. (2012). Color texture analysis based on fractal descriptors. *Pattern Recognition*, 45(5):1984–1992.

Cha, S.-H. and Srihari, S. N. (2002). On measuring the distance between histograms. *Pattern Recognition*, 35(6):1355–1370.

El Maliani, A. D., El Hassouni, M., Berthoumieu, Y., and Aboutajdine, D. (2014). Color texture classification method based on a statistical multi-model and geodesic distance. *Journal of Visual Communication and Image Representation*, 25(7):1717–1725.

Florindo, J. and Bruno, O. (2016). Texture analysis by fractal descriptors over the wavelet domain using a best basis decomposition. *Physica A: Statistical Mechanics and its Applications*, 444:415–427.

Guo, J.-M., Prasetyo, H., Lee, H., and Yao, C.-C. (2016). Image retrieval using indexed histogram of Void-and-Cluster Block Truncation Coding. *Signal Processing*, 123:143–156.

Guo, Y., Zhao, G., and Pietikäinen, M. (2012). Discriminative features for texture description. *Pattern Recognition*, 45(10):3834–3843.

Kalakech, M., Porebski, A., Vandenbroucke, N., and Hamad, D. (2015). A new LBP histogram selection score for color texture classification. In *Image Processing Theory, Tools and Applications (IPTA), 2015 International Conference on*, pages 242–247.

Lakmann, R. (1998). Barktex benchmark database of color textured images.

Ledoux, A., Losson, O., and Macaire, L. (2016). Color local binary patterns: compact descriptors for texture classification. *Journal of Electronic Imaging*, 25(6):061404.

Liu, M. and Zhang, D. (2014). Sparsity score: a novel graph-preserving feature selection method. *International Journal of Pattern Recognition and Artificial Intelligence*, 28(04):1450009.

Martínez, R. A., Richard, N., and Fernandez, C. (2015). Alternative to colour feature classification using colour contrast ocurrence matrix. In *The International Conference on Quality Control by Artificial Vision 2015*, pages 953405–953405. International Society for Optics and Photonics.

Mehta, R. and Egiazarian, K. (2016). Dominant Rotated Local Binary Patterns (DRLBP) for texture classification. *Pattern Recognition Letters*, 71:16–22.

Mäenpää, T. and Pietikäinen, M. (2004). Classification with color and texture: jointly or separately? *Pattern Recognition*, 37(8):1629–1640.

Ojala, T., Maenpaa, T., Pietikainen, M., Viertola, J., Kyllonen, J., and Huovinen, S. (2002a). Outex - new framework for empirical evaluation of texture analysis algorithms. In *Pattern Recognition, 2002. Proceedings. 16th International Conference on*, volume 1, pages 701–706 vol.1.

Ojala, T., Pietikäinen, M., and Harwood, D. (1996). A comparative study of texture measures with classification based on featured distributions. *Pattern Recognition*, 29(1):51 – 59.

Ojala, T., Pietikäinen, M., and Mäenpää, T. (2001). A Generalized Local Binary Pattern Operator for Multiresolution Gray Scale and Rotation Invariant Texture Classification. In *Proceedings of the Second International Conference on Advances in Pattern Recognition*, ICAPR '01, pages 397–406, London, UK, UK. Springer-Verlag.

Ojala, T., Pietikäinen, M., and Mäenpää, T. (2002b). Multiresolution Gray-Scale and Rotation Invariant Texture Classification with Local Binary Patterns. *IEEE Trans. Pattern Anal. Mach. Intell.*, 24(7):971–987.

Oliveira, M. W. d. S., da Silva, N. R., Manzanera, A., and Bruno, O. M. (2015). Feature extraction on local jet space for texture classification. *Physica A: Statistical Mechanics and its Applications*, 439:160–170.

Pietikäinen, M., Hadid, A., Zhao, G., and Ahonen, T. (2011). *Computer Vision Using Local Binary Patterns*, volume 40. Springer London, London.

Pietikäinen, M., Mäenpää, T., and Viertola, J. (2002). Color texture classification with color histograms and local binary patterns. In *Workshop on Texture Analysis in Machine Vision*, pages 109–112.

Porebski, A., Vandenbroucke, N., and Hamad, D. (2013a). LBP histogram selection for supervised color texture classification. In *ICIP*, pages 3239–3243.

Porebski, A., Vandenbroucke, N., and Macaire, L. (2013b). Supervised texture classification: color space or texture feature selection? *Pattern Analysis and Applications*, 16(1):1–18.

Porebski, A., Vandenbroucke, N., Macaire, L., and Hamad, D. (2014). A new benchmark image test suite for evaluating colour texture classification schemes. *Multimedia Tools and Applications*, 70(1):543–556.

Qazi, I.-U.-H., Alata, O., Burie, J.-C., Moussa, A., and Fernandez-Maloigne, C. (2011). Choice of a pertinent color space for color texture characterization using parametric spectral analysis. *Pattern Recognition*, 44(1):16–31.

Qiao, L., Chen, S., and Tan, X. (2010). Sparsity preserving projections with applications to face recognition. *Pattern Recognition*, 43(1):331–341.

Ren, J., Jiang, X., and Yuan, J. (2015). Learning LBP structure by maximizing the conditional mutual information. *Pattern Recognition*, 48(10):3180–3190.

Xu, J., Yang, G., Man, H., and He, H. (2013). L1 graph based on sparse coding for feature selection. In *Advances in Neural Networks–ISNN 2013*, pages 594–601. Springer.

Zhang, Q. and Xu, Y. (2015). Block-based selection random forest for texture classification using multifractal spectrum feature. *Neural Computing and Applications*.

Zhou, G., Lu, Z., and Peng, Y. (2013a). L1-graph construction using structured sparsity. *Neurocomputing*, 120(0):441 – 452.

Zhou, S.-R., Yin, J.-P., and Zhang, J.-M. (2013b). Local binary pattern (LBP) and local phase quantization (LBQ) based on Gabor filter for face representation. *Neurocomputing*, 116:260–264.

Zhu, X., Wu, X., Ding, W., and Zhang, S. (2013). Feature selection by joint graph sparse coding. In *SDM*, pages 803–811. SIAM.